Received: 21 February 2019

DOI: 10.1002/mop.32002

WILEY

RESEARCH ARTICLE

A low complexity spectrum shaping scheme for substrate integrated waveguides based on spread reshaping code

Yu Zhao | **Rainer Grünheid** | **Gerhard Bauch**

Institute of Communications, Hamburg University of Technology, Hamburg, Germany

Correspondence
Yu Zhao, Institute of Communications, Hamburg University of Technology, Eißendorfer Strasse 40, 21073, Hamburg, Germany.
Email: yu.zhao@tuhh.de

Abstract

In the microwave and millimeter-wave transmission regions, substrate-integrated waveguide (SIW) is a very promising candidate for the development of circuits and components. The channel of the SIW is a bandpass or high pass filter. This characteristic impedes the conventional baseband transmission using nonreturn-to-zero pulse shaping scheme. As an alternative to using mixers to facilitate a passband transmission, this paper proposes a spectrum shaping scheme of low complexity for the channel of SIW, namely spread reshaping code. It aims at matching the spectrum of the transmit signal to the channel frequency response. It facilitates the transmission through the SIW channel while it avoids using carrier modulation and equalization. Simulations reveal a good performance of this scheme, such that, as a result, eye opening is achieved without any equalization or modulation for the respective transmission channels.

KEYWORDS

bandpass channel, eye opening, spectrum shaping, spread reshaping code, substrate integrated waveguide, switching frequency

1 | INTRODUCTION

Substrate integrated waveguides (SIW) are a very promising candidate for the development of circuits and components in the microwave and millimeter-wave transmission regions.[1-5] In these regions, conventional microstrip or coplanar waveguides perform poorly in reaching a wide band transmission because of high conductor and dielectric losses at high frequencies. In comparison with them, an SIW can maintain a high quality factor, low insertion loss, and high power capacity at frequency ranges higher than 30 GHz.[1,3] Furthermore, it provides the possibility to integrate all the components on the same substrate, including passive components, active elements, and antennas.[3] One more advantage is that it involves a low power consumption and low-cost fabrication process.[4,5]

As shown in References 1-6 an SIW is a nonplanar waveguide whose sidewalls are formed by utilizing rows of metallic via holes. This structure suppresses the low frequency components and makes the channel of the SIW a band pass or high pass filter. This impedes the conventional baseband chip-to-chip communication using the nonreturn-to-zero (NRZ) pulse shaping Scheme,[6-8] because the energy of the NRZ signal is concentrated in the main lobe of the spectrum at low frequencies.

One straightforward solution of transmitting signals through the SIW channel is to use carrier modulation. As shown in References 6 and 8, mixers are proposed to be used as carrier modulator and demodulator in order to transmit the NRZ signal through the SIW channel. However, due to extremely tight constraints on power consumption and latency in high speed chip-to-chip communication, it is too complex and expensive to implement a carrier modulation system.

An alternative is to shape the signal spectrum and match it to the channel magnitude response. In Reference 7 we proposed Manchester coding and bipolar coding as the spectrum shaping schemes for the SIW channel. They facilitate the band pass transmission for the SIW channel given in Reference 7. However, if the lower cutoff frequency of the passband is higher than $1/T_s$ or $2/T_s$, where T_s is the duration of the transmitted symbol, these two schemes will perform poorly due to the mismatch between the spectrum and the channel response. Therefore, this paper proposes a spectrum shaping scheme of low complexity, namely spread reshaping

code (SRC). It shapes the signal spectrum by adjusting the switching frequency of the transistors at the transmitter. It facilitates the transmission through any SIW channel while avoid using carrier modulation. In some cases it even does not need equalization. Its suitability is demonstrated using exemplary SIW channel models. Note that that a shorter conference version of this idea is introduced briefly in Reference 9. This paper analyzes the principle of encoding/decoding much more deeply and comprehensively. Moreover, it compares the hardware complexity and provides additional simulation results.

The rest of the paper is organized as follows: Section 2 covers the model of chip-to-chip communication and the SIW channel. Section 3 proposes the spread reshaping code as a spectrum shaping solution for the SIW channel. Different codes are constructed based on a code construction algorithm. Their performance is assessed in terms of eye opening in distinct SIW channels. In Section 4, the complexity of the proposed scheme is compared with the conventional NRZ scheme. The conclusion is drawn in Section 5.

2 | CHANNEL MODEL

In this section, channel models regarding chip-to-chip communication and the SIW are presented in detail. The physical mechanisms of the SIW are explained in References 1-6.

In chip-to-chip communication systems there are many parallel channels between chips. A single channel model can be used to represent the data transmission links in case that the crosstalk is negligible. A state-of-the-art single channel transmission system of chip-to-chip communication is modeled in Figure 1. Bits are transmitted by the driver as rectangular pulses of width T_S over two electrical wires. The supply noise[10] and the simultaneous switching output (SSO) noise[11] are removed by utilizing differential signaling. The thermal noise is mostly negligible. Therefore the main impairment considered in the modeling is the ISI caused by the channel dispersion and reflections,[7] which are represented by impulse responses (IR) $h_1(t)$ and $h_2(t)$ in Figure 1.

At the receiver, the analog equalizers $w_{1,\,2}(t)$ partly compensate the degradations, and a comparator calculates the differences between the two received signals $y_1(t)$ and $y_2(t)$. The differences between $y_1(t)$ and $y_2(t)$ is expressed as

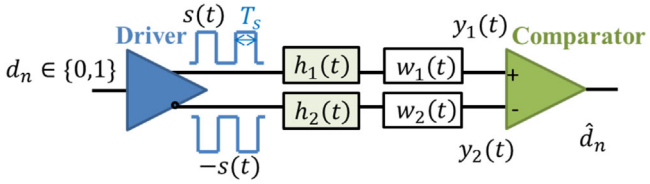

FIGURE 1 Single channel transmission system of chip-to-chip communication [Color figure can be viewed at wileyonlinelibrary.com]

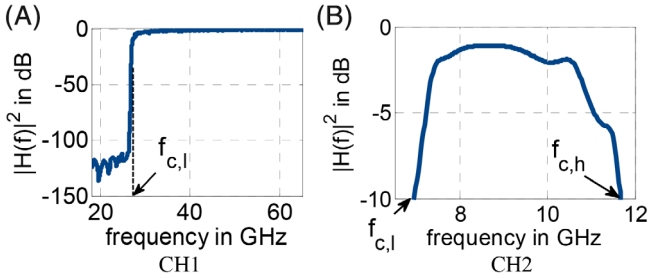

FIGURE 2 Channel models, the circuit parameters are explained in References 5 and 12: A, a high pass channel measured in Reference 12; B, a band pass channel measured in Reference 5 [Color figure can be viewed at wileyonlinelibrary.com]

$$y_1(t) - y_2(t) = s(t)*[h_1(t)*w_1(t) + h_2(t)*w_2(t)], \qquad (1)$$

where * stands for convolution, and $h_1(t) \approx h_2(t)$.

Using the proposed spectrum shaping schemes in this paper, equalization can be avoided in the tested scenarios. This will be the simulation setup in this paper. Since the main problem of the SIW channel stems from its band pass or high pass channel characteristic, the investigation on the channel model of an SIW will focus on the transfer function $H(f)$ instead of on the impulse response $h(t)$. Figure 2A presents a high pass channel measured in Reference 12 where the 10 dB lower cutoff frequency $f_{c,\,1}$ is around 27 GHz. Note that, physically, a high pass channel will have its higher cutoff frequency and become a band pass channel. Figure 2B depicts a measured band pass channel with 10 dB cutoff frequencies of around 7 and 11.6 GHz,[5] where $f_{c,\,l}$, $f_{c,\,h}$ stand for the lower and higher cutoff frequencies, respectively.

In this paper, the performance of spectrum shaping is analyzed in terms of eye opening. The eye opening of the conventional NRZ scheme under a band pass channel is shown in our study in Reference 7, where $f_{c,\,1}$= 1.6 GHz. It is found that the significant loss of signal power during the transmission leads to serious eye closing of the NRZ signal. For the channels in Figure 2, where $f_{c,\,1}$ is much higher than that in Reference 7, the performance will be even worse because more power will be lost during transmission. To reduce the power loss, suitable transmission schemes have to be identified.

3 | SPREAD RESHAPING CODE

In this section, to solve the aforementioned problems of the SIW channel, a spectrum shaping technique named spread reshaping code is proposed.

There are many methods to shape the signal spectrum in wireless communications. However, under the extreme tight constraints on energy consumption and latency, these conventional methods are undesired in commercialized chip-to-chip communication. What can be manipulated at the

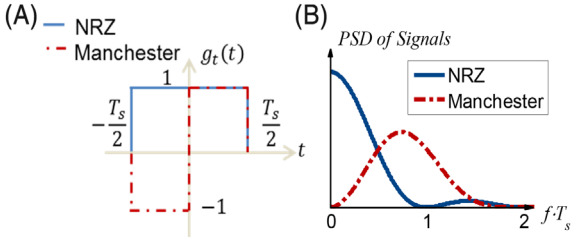

FIGURE 3 A, Pulse shape and B, PSD of Manchester coding and NRZ. NRZ, nonreturn-to-zero; PSD, power spectrum density [Color figure can be viewed at wileyonlinelibrary.com]

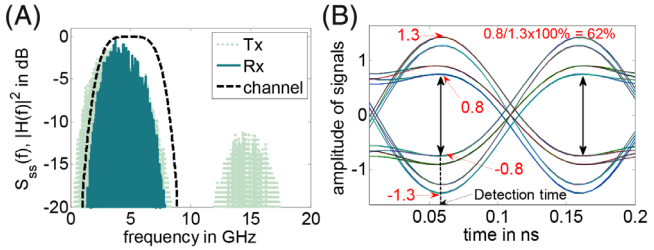

FIGURE 4 Performance of Manchester coding in case of the band pass channel in Reference 7, at the data rate of 5 Gbit/s. A, signal PSD $S_{ss}(f)$, channel response $|H(f)|^2$; B, eye diagram with two sub-eyes. PSD, power spectrum density [Color figure can be viewed at wileyonlinelibrary.com]

transmitter is mainly the switching frequency of the transistors. Considering these constraints, we propose the spread reshaping code, which shapes the spectrum by adjusting the switching frequency of the transistors.

3.1 | Manchester coding, a special case of spread reshaping code

Manchester coding as used in Reference 7, is the simplest case of the proposed spread reshaping code, hence in this section it will be introduced as an example for an easier understanding. The Manchester pulse shape is depicted by the dashed-dot line in Figure 3A, where the NRZ pulse shape is represented by the solid line as a comparison. According to IEEE 802.3, Manchester coding represents binary information by a rising or falling edge of a rectangular pulse in the center of each symbol interval. A rising edge denotes an information bit of one, whereas a falling edge characterizes a zero.

In this paper, the shape of power spectrum density (PSD) is depicted by $|G_t(f)|^2$, because PSD is proportional to $|G_t(f)|^2$, where $G_t(f)$ is the Fourier transform of $g_t(t)$. Based on the Manchester pulse shape $g_t(t)$, it can be derived that the PSD of Manchester coding is represented by

$$|G_t(f)|^2 = \left| T_s \mathrm{si}\left(\frac{\pi}{2} f T_s\right) \sin\left(\frac{\pi}{2} f T_s\right) \right|^2, \quad (2)$$

where the si function is defined as $\mathrm{si}(x) = \sin(x)/x$. The corresponding shapes of PSD are depicted in Figure 3B. It can be seen that due to the function $\sin\left(\frac{\pi}{2} f T_s\right)$, the low frequency components do not carry significant power. The spectrum has a band pass characteristic in the interval $[0, 2/T_s]$, which matches the band pass channel of the SIW better than the NRZ pulse. The additional cost associated with Manchester coding is the doubling of the switching frequency of transistors at the transmitter, such that two "sub-eyes" should be distinguished in one sampling interval.

As a comparison to the NRZ scheme under the bandpass channel in Reference 7, the performance of Manchester coding is shown in this paper in Figure 4, where Tx stands for transmitter and Rx means receiver. The gray dotted lines represent the power spectral density (PSD) $S_{ss}(f)$ of the transmitted signal, the solid dark green lines are the PSD of the received signal and the dashed black curve shows the square of the channel magnitude response $|H(f)|^2$. In Figure 4 it can be seen that matching the spectrum to the channel, two wanted sub-eyes are distinguished in one sampling interval, the opening eye height of the best sub-eye is $[-0.8\ 0.8]$. Approximately 62% vertical opening is obtained without any equalization.

Further simulations show that Manchester coding facilitates the transmission at data rates from 3 to 8 Gbit/s under this band pass channel. Furthermore, the simulations reveal that if the lower cutoff frequency of the passband is higher than $1/T_s$, this code will perform poorly due to the mismatch between the spectrum and the channel response. Such as in the channel case of Figure 2A,B, using Manchester coding will not be able to facilitate the transmission without complex equalizers. To cope with this problem, the spread reshaping code is proposed.

3.2 | Principle of spread reshaping code

Mathematically speaking the pulse shaping procedure of Manchester coding is to multiply the message signal $d(t)$ by a spreading sequence $c(t)$, $s(t) = d(t) \times c(t)$, where $s(t)$ is the shaped signal. The elements of the spreading sequence $c(t)$ are called chips c_k with chip duration T_c and chip rate $1/T_c$. Moreover, $S = T_s/T_c$ is defined as spreading factor. For instance, using Manchester coding as shown in Figure 3A, the chip sequence $[c_1, c_2] = [-1, 1]$, $T_c = T_s/2$, and $S = 2$.

Following this lead, the encoding principle of the spread reshaping code is depicted in Figure 5. A pulse shape $g_t(t)$ will be designed considering the desired data rate and the channel condition. Designing a pulse shape $g_t(t)$ is equivalent to designing an encoder using a specific spreading factor S and a deterministic chip sequence $c_k = [c_1, c_2 \ldots c_s]$, $c_k \in \{\pm 1\}$. An example is shown in Figure 5, where the deterministic chip sequence c_k=[1 −1 1 −1] and the spreading factor S=4.

Since the chips apply rectangular pulse, the pulse shape of the spread reshaping code can be expressed as

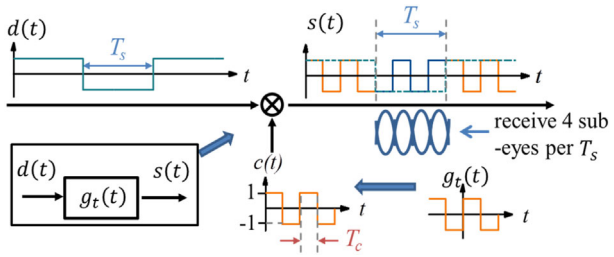

FIGURE 5 Encoding of the spread reshaping code in the time domain [Color figure can be viewed at wileyonlinelibrary.com]

$$g_t(t)=\begin{cases}\sum_{k=0}^{2n-1} c_k\cdot \mathrm{rect}\left(\frac{t}{T_c}-k+n-\frac{1}{2}\right), \\ \qquad n\in\mathbb{N}\ \text{for}\ S=2n, \\ \sum_{k=0}^{2n} c_k\cdot \mathrm{rect}\left(\frac{t}{T_c}-k+n\right), \\ \qquad n\in\mathbb{N}\ \text{for}\ S=2n+1,\end{cases} \tag{3}$$

The corresponding spectrum is

$$G_t(f)=\begin{cases}T_c\mathrm{si}(\pi f T_c)\sum_{k=0}^{2n-1} c_k\cdot e^{-j[2(k-n)+1]\pi f T_c}, \\ \qquad n\in\mathbb{N}\ \text{for}\ S=2n, \\ T_c\mathrm{si}(\pi f T_c)\sum_{k=0}^{2n} c_k\cdot e^{-j2(k-n)\pi f T_c}, \\ \qquad n\in\mathbb{N}\ \text{for}\ S=2n+1.\end{cases} \tag{4}$$

From Equation (4) it can be seen that the shape of $G_t(f)$ is determined by two elements, the first one is the function $si(x) = \sin(x)/x$, and the second one is

$$\sum e^{j\varphi}\pm e^{-j\varphi}\sim\sum\sin(\varphi)\pm\sum\cos(\varphi),$$
$$\varphi=[2(k-n)+1]\pi f T_c \text{ or } 2(k-n)\pi f T_c, \tag{5}$$

where the exponent of the exponential function in Equation (4) is substituted by φ. The main lobe of $si(\pi f T_c)$ function in Equation (4) is used to spread the spectrum to $[-1/T_c, 1/T_c]$ in order to cover the passband of the channel. Meanwhile, the combination of sin and cos functions from Equation (5) reshapes the spread spectrum to match the channel magnitude response.

At the receiver up to S sub-eyes will be received, where two methods can be applied for decoding. As shown in Figure 6, the first one is detecting using a threshold detector directly at the time of the biggest vertical opening eye among all sub-eyes,

$$\hat{d}_n=\mathrm{sign}[y(n\times T_s-T_0)], n\in\mathbb{N}, \tag{6}$$

where T_0 indicates the detection time within T_s. An example of this "best detection time" is shown in the two "sub-eyes"

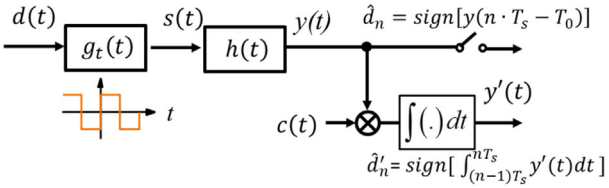

FIGURE 6 Decoding methods of the spread reshaping code [Color figure can be viewed at wileyonlinelibrary.com]

in Figure 4B, where the best detecting time corresponds to the arrows pointing to the amplitudes of ±0.8. This method is simple and fast enough to support a high throughput. However, in case that the vertical opening differences between the biggest sub-eye and other sub-eyes are large, the random noise tolerance of the code will be reduced.

The second decoding algorithm is based on despreading method of the direct sequence spread spectrum technique. As shown in Figure 6, the received signal $y(t)$ will be multiplied with the spreading sequence $c(t)$ and integrated over one symbol interval.

$$\hat{d}'_n=\mathrm{sign}\left[\int_{(n-1)T_s}^{nT_s} y(t)\times c(t)dt\right] \tag{7}$$

This method exploits the information of all the sub-eyes fully, such that the random noise tolerance is increased. However, the complexity and energy consumption are raised as well due to the multiplication and the integration. Since the random thermal noise is nearly negligible, and the ISI dominates the channel impairments, the first decoding method (6) will be used to demonstrate the performance in the following sections.

3.3 | Code construction algorithm

In order to match the main lobe of the spectrum with the pass band of the channel as much as possible, a proper combination of the spreading factor S($S\in\mathbb{N}$, $S\geq 2$) and the code sequence $c_k\in\{\pm 1\}$ is needed. This is realized through a code construction algorithm, which searches the optimum parameter combination based on a cost function f_{SRC}

$$f_{SRC}=1-\frac{\int|s(t)*h(t)|^2dt}{\int|s(t)|^2dt}, \tag{8}$$

where $\int|s(t)*h(t)|^2dt$ stands for the received signal power after channel filtering, $\int|s(t)|^2dt$ is the transmitted signal power. f_{SRC} shows the remaining power ratio after transmission. It demonstrates the match degree between the shaped spectrum and the channel magnitude response. This function is derived using the "water-filling" formula based on the theorem of the Shannon capacity of time-invariant frequency-selective fading channels.[13] The algorithm aims at minimizing the cost function f_{SRC} by searching for the optimum S and c_k in a given range of $[S_{min}, S_{max}]$, under a target data

rate T_s. Using this code, at least one of the "sub-eyes" should be distinguished in one sampling interval of duration T_s at the receiver. One example of S "sub-eyes" is shown in Figure 4B where $S = 2$. The drawback of this code is that it is more sensitive to sampling time jitter than the NRZ scheme.

3.4 | Performance of spread reshaping code in a bandpass channel

The performance of the spread reshaping code is assessed in the channel case of Figure 2B. To match this channel, the search range in the construction algorithm is set to $3 \le S \le 10$, the target data rate is 4 Gbit/s and the cost function is set to $f_{SRC} \le 70\%$ in the construction. The optimum combination of S and c_k is found to be $S = 8$, $c_k = [-1\ 1\ 1\ -1\ -1\ 1\ 1\ -1]$. This code is denoted as spread reshaping code 1 (SRC1). The pulse shape $g_t(t)$ of SRC1 is depicted in Figure 7A. It can be derived from $g_t(t)$ that five sub-eyes will be transmitted.

The PSD corresponding to the pulse shape $g_t(t)$ can be represented as

$$|G_t(f)|^2 = \left|\frac{2}{\pi f}\left[\sin\left(\frac{3\pi}{4}fT_s\right) - \sin\left(\frac{\pi}{4}fT_s\right) - \frac{1}{2}\sin(\pi fT_s)\right]\right|^2, \quad (9)$$

which yields a PSD shape as depicted by the orange dashed curve in Figure 7C. This PSD is located mainly in the interval $[1/T_s, 3/T_s]$, that means when $T_s = 2.5$ ns, the main lobe of the spectrum will concentrate between 4 and 12 GHz. This matches the passband of the channel in Figure 2B.

Figure 8A,B shows the performance of the spread reshaping code 1 (SRC1) in case of channel Figure 2B, namely CH2, at the data rate of 4 Gbit/s. The spectrum in Figure 8A

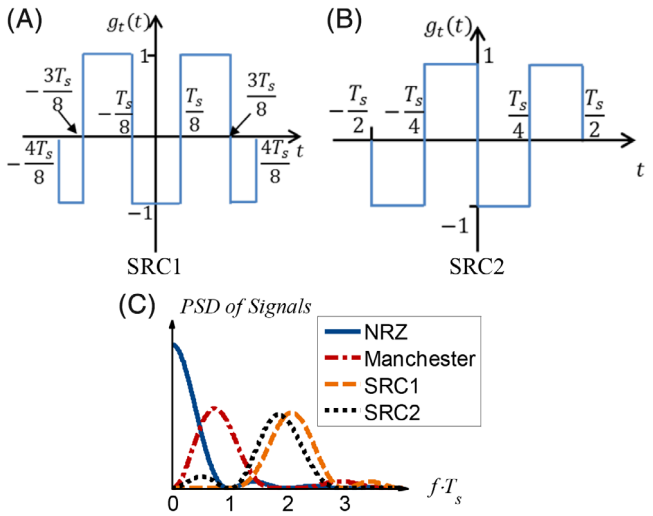

FIGURE 7 A,B, Pulse shape and C, PSD of spread reshaping codes. PSD, power spectrum density [Color figure can be viewed at wileyonlinelibrary.com]

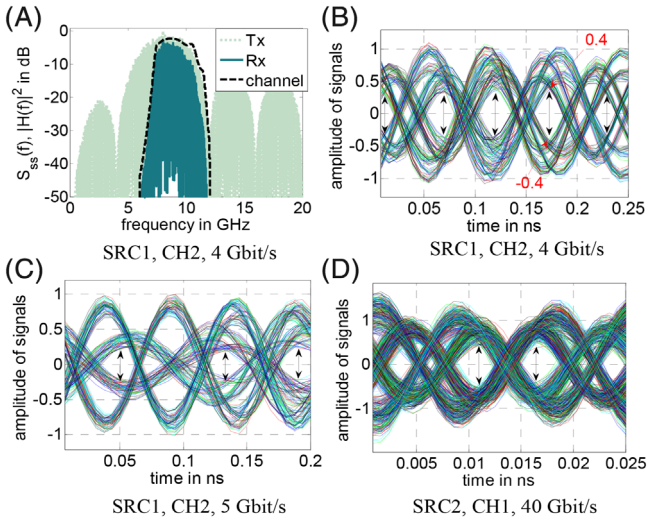

FIGURE 8 Performance of spread reshaping code in cases of channel Figure 2A,B, namely CH1 and CH2. A, SRC1, CH2, 4 Gbit/s; B, SRC1, CH2, 4 Gbit/s; C, SRC1, CH2, 5 Gbit/s; D, SRC2, CH1, 40 Gbit/s. SRC1, spread reshaping code 1; SRC2, spread reshaping code 2 [Color figure can be viewed at wileyonlinelibrary.com]

shows that, transmitting the data at the rate of 4 Gbit/s, the main lobe of the spectrum occupies the desired frequencies between 4 and 12 GHz, such that around 30% of the signal energy is preserved after transmission. From the eye-diagram in Figure 8B it can be seen that the wanted five sub-eyes can be distinguished clearly, approximately 40% vertical opening is achieved without any equalization.

To investigate the data rate tolerance of this coding scheme, the target data rate is increased from 4 to 5 Gbit/s in the code construction algorithm. Under the limitations of $3 \le S \le 10$ and $f_{SRC} \le 75\%$, the algorithm delivers the same code parameters as SRC1. Transmitting this code at 5 Gbit/s the power loss of the signal spectrum is raised by about 5% points. This leads to two closed sub-eyes in the received eye diagram, as shown in Figure 8C. The other three sub-eyes remain open by about 25% vertically.

To reduce the sensitivity of this code to the sampling time jitter, a tradeoff is made between the eye opening and the switching frequency. The search range of S is set to $3 \le S \le 4$, and $f_{SRC} \le 75\%$, data rates are 4∼5 Gbit/s. The construction algorithm delivers the parameter combination of $S = 4$, $c_k = [-1\ 1\ -1\ 1]$. This code is denoted as spread reshaping code 2 (SRC2). The pulse shape of SRC2 is depicted in Figure 7B. It can be derived from $g_t(t)$ that four sub-eyes will be transmitted. The squared magnitude response $|G_t(f)|^2$ of signals corresponding to the pulse shape $g_t(t)$ of SRC2 is

$$|G_t(f)|^2 = \left|\frac{T_s}{2}\mathrm{sinc}\left(\frac{\pi}{4}fT_s\right)\left[\sin\left(\frac{3\pi}{4}fT_s\right) - \sin\left(\frac{\pi}{4}fT_s\right)\right]\right|^2, \quad (10)$$

which yields a PSD of black dotted curve in Figure 7C.

Applying this code at the data rate of 5 Gbit/s in case of channel Figure 2B, the performance is similar as that of SRC1. In the simulation about 28% vertical eye opening is achieved without any equalization. However, in transmission at the data rate of 4 Gbit/s, the obtained eye-opening is half of the one of SRC1 (in Figure 8B). Hence the noise tolerance of SRC2 is reduced. This is the compromise for reducing the switching frequency. However, the time jitter tolerance and energy efficiency of SRC2 is better than that of SRC1. In case that the constraint on the overall complexity is high, and the random thermal noise is negligible, SRC2 is preferred rather than SRC1.

In further simulations it is found that for other band pass channels of the SIW, the main lobe of the spectrum can be shifted to any frequency ranges of $[N_1/T_s, N_2/T_s]$, N_1, $N_2 \in \mathbb{R}$, $N_1 \geq 0$, $N_2 \geq 1$. Considering the energy consumption constraint as well as the sensitivity to the time jitter, a tradeoff should be made between the performance and the allowable switching frequency.

3.5 | Performance of spread reshaping code in a high pass channel

Some SIW channels have typically a high pass characteristic instead of bandpass,[6,8,12] as the sample channel shown in Figure 2A. In this case it will be even easier to transmit the data at higher rates than in the band pass channel of last section, as long as the main lobe of the spectrum is reshaped to the pass band. Using the construction algorithm and setting $2 \leq S \leq 4$, and $f_{SRC} \leq 75\%$, targeting the data rate of 15∼40 Gbit/s in the high pass channel in Figure 2A, the construction algorithm delivers the a spread reshaping code of $S = 4$, $c_k = [-1\ 1\ -1\ 1]$, which is actually the spread reshaping code 2 (SRC2). Further code construction and simulations at data rates up to 200 Gbit/s are carried out in high pass channels. It is found that using the spread reshaping code, the bigger the data rate is, the less energy will be lost during the transmission, and a better eye opening will be obtained. This is because the main lobe moves toward the high frequency range along with the increase in data rate, which fits for the high pass characteristics of the channel. Figure 8D shows the eye diagram of SRC2 at the data rate of 40 Gbit/s. In this case the main lobe of the spectrum locates mostly in the passband, such that 46% of the signal power is preserved after transmission. Thus, a vertical eye opening of around 42% is obtained. It is also found that in transmission at data rates higher than 40 Gbit/s, using spreading factor S=2 will deliver a distinguishable opened eye diagram. This reduces further the requirements on the switching frequency.

In practical cases, the pass band of the high pass channel will have degradations at high frequencies,[6,8,12] and have an upper cutoff frequency. The tractable data rates will then be determined both by the channel bandwidth and the allowable switching frequency.

4 | COMPLEXITY COMPARISION

In this section, the complexity of the SRC scheme will be compared with the scheme of NRZ plus mixer (noted as NRZ).

To realize a conventional coding scheme, encoder/decoder blocks have to be implemented. This can be avoided using the spread reshaping code. It can be seen from the last section that the principle of the SRC is to design a suitable pulse shape to replace the NRZ. From the pulse shapes in Figures 3 and 7 it can be derived that the encoder is nothing else than manipulating the switching rules of transistors at the transmitter. For instance, using the NRZ scheme, a transistor will be switched on to transmit a digit "1" and switched off to transmit a "0." Using the SRC in Figure 3, a transistor will be switched off and on in one T_s to transmit a digit "1," be switched on and off to transmit a "0." Thus, an encoder block is not needed. Furthermore, a decoder block is not needed either since we use the first decoding method (6).

The complexity of the SRC and NRZ schemes are compared in Table 1. In comparison with the NRZ scheme, the great advantage of the SRC scheme is that it does not need modulators at the transmitter or receiver. This avoids the power consumption on high frequency modulation/de-modulation. Furthermore, this provides the possibility to integrate all the components on a same substrate. However, using the SRC the switching frequency of the transistor at the transmitter is increased significantly. The SRC scheme requires a bandpass driver, while the NRZ scheme requires a low pass one. Note that in some optimized scenarios the NRZ scheme also needs a bandpass driver after the mixer.[8] The overall hardware complexity of the SRC scheme is lower, since no mixer or local oscillator is needed. More solid comparisons on the power consumption will need measurements on practical circuits, which will be carried out in our future work.

Note that the proposed SRC scheme is designed for a band pass channel, such as the SIW. In conventional microstrip transmission lines where the channel is low pass, the SRC scheme will perform worse than the NRZ scheme, since the spectrum shape of the NRZ signal matches the low pass channel characteristic better. For a low pass channel, a spectrum shaping scheme named duobinary signaling was

TABLE 1 Complexity comparison

Scheme	SRC	NRZ
Mixers, local oscillator	Not need	Need
Integration	Good	The oscillator is not integrated in a chip
Driver	Bandpass	Low pass/bandpass
Switching frequency of transistor	High	Low

Abbreviations: NRZ, nonreturn-to-zero; SRC, spread reshaping code.

analyzed in Reference 7 as an alternative to improve the spectrum efficiency.

5 | CONCLUSION

The band pass and high pass channel characteristics of the SIW are analyzed in this paper. To solve the problem of significant power loss of baseband transmission using NRZ signals in the SIW channel, a spectrum shaping scheme named spread reshaping code is proposed and analyzed comprehensively. It aims at matching the spectrum of the signal with the channel magnitude response while having a low overall complexity, since the carrier modulation and equalization can be avoided for the investigated scenarios. The cost is the significantly increased switching frequency of the transistor at the transmitter. To facilitate the optimum spectrum shaping to match the band pass or high pass SIW channel, a code construction algorithm is proposed to optimize the parameters of the spread reshaping code. It is designed based on the remaining power ratio after channel filtering. Note that there are other functions available for code construction, such as the received bit error rate, the eye opening percentage and so on. The propose function has the lowest computational complexity than other investigated functions. Simulations reveal that data rates from 5 to 200 Gbit/s are facilitated by this code without modulation or equalization for the respective SIW channels. It is found that the spread reshaping code can shape the spectrum into any interval between $[N_1/T_s, N_2/T_s]$, $N_1, N_2 \in \mathbb{R}$, $N_1 > 0$, $N_2 \geq 1$. However, a higher switching frequency consumes more energy. Moreover, the bigger the spreading factor S is the more sensitive the signal to time jitter will be. Thus, a tradeoff should be made between the performance and the allowable switching frequency. In the complexity comparison, it is found that the overall hardware complexity of the SRC scheme is lower than that of the NRZ plus mixers scheme. More solid comparisons will be carried out on the power consumption and energy efficiency of the two schemes in our future work.

ORCID

Yu Zhao https://orcid.org/0000-0002-0868-4377

REFERENCES

[1] Martinez JA, de Dios JJ, Belenguer A, Esteban H, Boria VE. Integration of a very high quality factor filter in empty substrate-integrated waveguide at Q-band. *IEEE Microw Wirel Compon Lett*. 2018;28(6):503-505.

[2] Chu P, Zheng K, Xu F. A planar diplexer using hybrid substrate integrated waveguide and coplanar waveguide. Paper presented at: 2017 IEEE 17th International Conference on Ubiquitous Wireless Broadband (ICUWB), 2017:1-4.

[3] Bozzi M, Georgiadis A, Wu K. Review of substrate-integrated waveguide circuits and antennas. *Antennas Propag IET Microw*. 2011;5(8):909-920.

[4] Park WY, Lim S. Miniaturized substrate integrated waveguide (SIW) bandpass filter loaded with double-sided-complementary split ring resonators (DS-CSRRs). Paper presented at: Microwave Conference (EuMC), 2011 41st European, 2011:740-743.

[5] Preibisch JB, Hardock A, Schuster C. Physics-based via and waveguide models for efficient SIW simulations in multilayer substrates. *IEEE Trans Microw Theory Tech*. 2015;63(6):1809-1816.

[6] Li Z, Mahani MS, Abhari R. Experiment of substrate integrated waveguide interconnect measurement for high speed data transmission application. *Microw Opt Technol Lett*. 2012;54(2):401-405.

[7] Zhao Y, Gruenheid R, Bauch G, Reuschel T, Schuster C. Redundant and non-redundant spectrum shaping schemes for reflection-limited chip-to-chip communication. Paper presented at: SCC 2017; 11th International ITG Conference on Systems, Communications and Coding, 2017:1-6.

[8] Mahani MS, Abhari R. Experimental evaluation of flexible high-speed interconnect system using substrate integrated waveguide technology. *Electron Lett*. 2012;48(23):1500-1501.

[9] Zhao Y, Gruenheid R, Bauch G. An energy efficient spectrum shaping scheme for substrate integrated waveguides. Paper presented at: *SPI 2019; IEEE 16th Workshop on Signal and Power Integrity*, 2019:1-4.

[10] Jovanovic MM. *Power Supply Technology—Past, Present, and Future*. Stuttgart: Mesago PCIM GmbH; 2007.

[11] Ding L, Mazumder P. Simultaneous switching noise analysis using application specific device modeling. *IEEE Trans Very Large Scale Integr VLSI Syst*. 2003;11(6):1146-1152.

[12] Simpson JJ, Taflove A, Mix JA, Heck H. Substrate integrated waveguides optimized for ultrahigh-speed digital interconnects. *IEEE Trans Microw Theory Tech*. 2006;54(5):1983-1990.

[13] Goldsmith A. *Wireless Communications*. Stanford California: Cambridge University Press; 2005:113-115.

How to cite this article: Zhao Y, Grünheid R, Bauch G. A low complexity spectrum shaping scheme for substrate integrated waveguides based on spread reshaping code. *Microw Opt Technol Lett*. 2020;62:93–99. https://doi.org/10.1002/mop.32002